Determination of pK_a Values of Carboxyl Groups in the N-Terminal Domain of Rat CD2: Anomalous pK_a of a Glutamate on the Ligand-Binding Surface[†]

Ho Ann Chen,[‡] Mark Pfuhl,[‡] Mark S. B. McAlister,[‡,§] and Paul C. Driscoll*[,‡,||]

Department of Biochemistry and Molecular Biology, University College London, Gower Street, London WC1E 6BT, U.K., and Ludwig Institute for Cancer Research, 91 Riding House Street, London W1P 8BT, U.K.

Received September 22, 1999; Revised Manuscript Received February 8, 2000

ABSTRACT: The ligand-binding surface of the T-lymphocyte glycoprotein CD2 has an unusually high proportion of charged residues, and ionic interactions are thought to play a significant role in defining the ligand specificity and binding affinity of CD2 with the structurally homologous ligands CD48 (in rodents) and CD58 (in humans). The determination of the electrostatic properties of these proteins can therefore contribute to our understanding of structure−activity relationships for these adhesion complexes that underpin T-cell adhesion to antigen-presenting cells. In this study, we investigated the pH titration behavior of the carboxyl groups of the N-terminal domain of rat CD2 (CD2d1) using the chemical shifts of backbone amide nitrogen-15 (^{15}N) and proton NMR resonances, and carboxyl carbon-13 (^{13}C) signals. The analysis revealed the presence of a glutamate (Glu41) on the binding surface of rat CD2 with an unusually elevated acidity constant (pK_a = 6.73) for CD2d1 samples at 1.2 mM concentration. pH titration of CD2d1 at low protein concentration (0.1 mM) resulted in a slight decrease of the measured pK_a of Glu41 to 6.36. The ionization of Glu41 exhibited reciprocal interactions with a second glutamate (Glu29) in a neighboring location, with both residues demonstrating characteristic biphasic titration behavior of the carboxyl ^{13}C resonances. Measurements at pH 5.5 of the two-bond deuterium isotope shift for the ^{13}C carboxyl resonances for Glu41 and Glu29 [$^2\Delta C^{\delta}(O^{\epsilon}D)$ = 0.2 and 0.1 ppm, respectively] were consistent with the assignment of the anomalous pK_a to Glu41, under the strong influence of Glu29. The characterization of single site mutations of CD2d1 residues Glu41 and Glu29 to glutamine confirmed the anomalous pK_a for Glu41, and indicated that electrostatic interaction with the Glu29 side chain is a significant contributing influence for this behavior in the wild-type protein. The implications of these observations are discussed with respect to recent structural and functional analyses of the interaction of rat CD2 with CD48. In particular, CD2 Glu41 must be a candidate residue to explain the previously reported strong pH dependence of binding of these two proteins in vitro.

The T-cell antigen CD2 is one of the best characterized of all the molecules involved in cell adhesion and cell−cell recognition (*1*−*5*). CD2 is involved in the adhesion interaction between T-cells and antigen-presenting target cells, and it appears to facilitate the dynamic interaction of T-cell receptor (TCR)[1] and antigen-loaded major histocompatibility complex (MHC) proteins by separating the cells at an optimal distance at the spatially segregated adhesion and signaling within what has been called the "immunological synapse" (*6*−*8*). CD2 may also be directly implicated in transmembrane signaling during T-cell activation (*1*, *2*, *9*). The physiological binding partner of CD2 has been shown to be CD48 in rodents (*10*, *11*) and CD58 in humans (*12*, *13*). The relatively low binding affinity of the interaction of CD2 with its ligand differs significantly from the well-characterized high-affinity protein−protein interactions of many soluble proteins and antigen−antibody complexes. This type of intermolecular association, which is characteristic of many cell-adhesion molecules, has been suggested to be essential to maintain the transient, reversible, and highly dynamic interaction between T-lymphocytes and antigen-presenting target cells (*14*, *15*). In general, the dissection of the binding characteristics of these proteins should provide valuable insight into the physicochemical basis of cell−cell adhesion, and therefore the biochemical and biophysical properties of CD2 have been the subject of a number of studies in recent years (*15*−*20*).

CD2 is comprised of two extracellular immunoglobulin superfamily (IgSF) domains and an intracellular C-terminal

[†] Grant support was provided by the Royal Society (P.C.D.), the European Molecular Biology Organization (M.P.), and the British Biosciences and Biotechnology Research Council (P.C.D. and M.S.B.M.). This is a contribution from the Bloomsbury Centre for Structural Biology supported by the BBSRC.

* To whom correspondence should be addressed at the Department of Biochemistry and Molecular Biology, University College London, Gower St., London WC1E 6BT, U.K. E-mail: driscoll@biochem.ucl.ac.uk, Tel.: +44-20 7679 7035, Fax: +44-20 7679 7193.

[‡] University College London.

[§] Present address: Department of Crystallography, Birkbeck College, Malet St., London WC1E 7HX, U.K.

[||] Ludwig Institute for Cancer Research.

[1] Abbreviations: 2D, two-dimensional; CD2d1, CD2 domain 1; EDTA, ethylenediaminetetraacetic acid; HSQC, heteronuclear single quantum coherence; IgSF, immunoglobulin superfamily; MHC, major histocompatibility complex; NMR, nuclear magnetic resonance; NOE, nuclear Overhauser effect; PCR, polymerase chain reaction; PMSF, phenylmethylsulfonyl fluoride; ppm, parts per million; TCR, T-cell receptor.

10.1021/bi992209z CCC: $19.00
Published on Web 05/19/2000

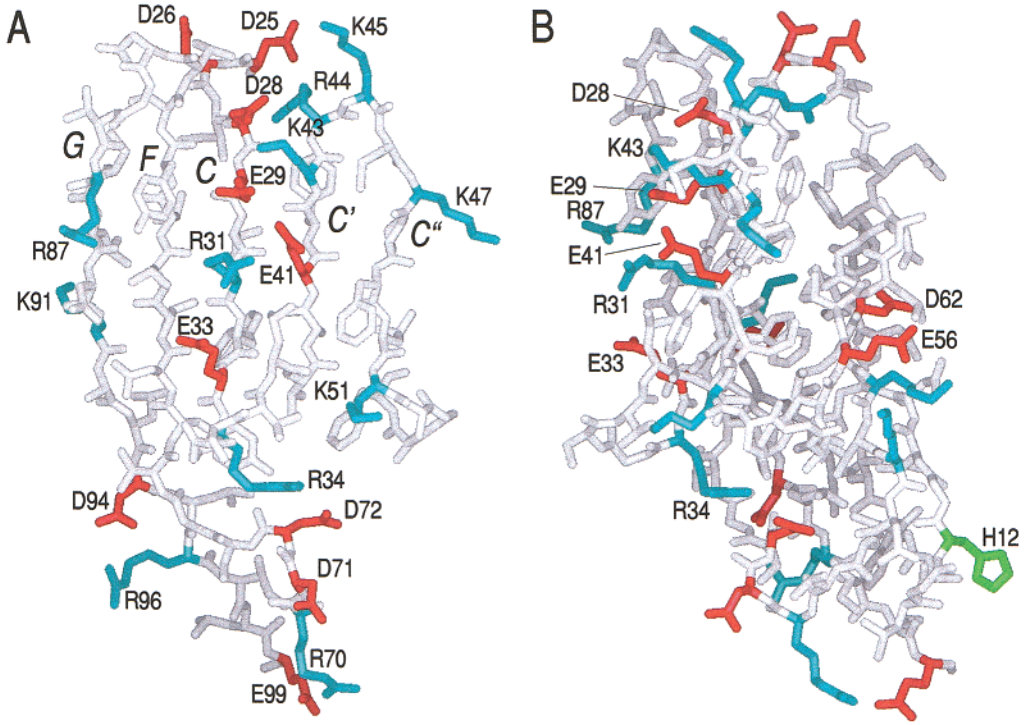

FIGURE 1: Structure of rat CD2 domain 1 illustrating (A) a face-on view of the major β-sheet ligand-binding surface of the domain, the flat nature of which is emphasized in the side-on view of the whole domain in (B). The atomic coordinates used are derived from the X-ray structure of the rat CD2 ectodomain (Protein Data Bank code 1HNG). Charged residues are colored according to the following scheme: arginine and lysine, blue; aspartic acid and glutamic acid, red; and histidine, green. The characteristic β-strand labeling (strands C″, C′, C, F, and G) is indicated in (A).

domain linked by a single transmembrane helix. It has been shown that the adhesion function of CD2 resides solely in the N-terminal domain, denoted CD2d1 (*21*−*23*). The structure of the CD2 ectodomain has been determined by X-ray crystallography (*24*, *25*), and the solution structures of the isolated N-terminal domain have been examined in detail by NMR spectroscopy (*26*, *27*), for both rat and human forms. CD2, together with its structurally homologous adhesion ligands CD48 and CD58, forms a subset of molecules within the IgSF that is suggested to have evolved from a common precursor involved in primordial homophilic interactions (*28*, *29*). A putative model of such homophilic interaction can be observed in the packing within crystals of both rat and human CD2, each of which exhibits a head-to-head homodimer interaction with extensive lattice contacts involving the N-terminal domain GFCC′C″ β-sheet (*24*, *25*). The characteristics of the crystal contact have also been put forward as a model for the physiological heterophilic association of CD2 and CD48 (*24*). Evidence to support this model has been provided by a number of experimental studies using mutational analysis (*7*, *15*, *30*) and NMR spectroscopy (*16*) which identified the CD2 residues implicated in CD48 binding. These residues form a contiguous binding "patch" that extends across an area that corresponds closely to the crystal contact. Most recently, Reinherz, Wagner, and colleagues have made a significant advance in the analysis of human CD2−human CD58 interactions by NMR spectroscopic examination of the structure of a highly mutated soluble form of CD58 domain 1 (*31*) and the co-crystallization of the CD58 domain with a mutated form of human CD2 domain 1 (*32*). The structure observed for the human CD2/CD58 complex, which is presumed to be homologous to that of rat CD2/CD48, possesses the basic features predicted by the previous models proposed on the basis of mutagenesis studies and the lattice contacts in the crystals of CD2 alone.

The dissociation constant (K_D) for CD2 interaction with its ligands has been determined to be 10−20 μM for human CD2/CD58 (*33*) and 60−90 μM for rat CD2/CD48 (*34*), with an exceptionally fast off-rate of ∼7.8 s^{-1} for rat CD2 (*17*). These weak interactions of CD2 are nevertheless highly specific. The binding sites of human and rat CD2 possess broadly similar characteristics, but these proteins demonstrate little cross-species binding to the respective ligands: human CD2 does not bind rat CD48, and rat CD2 does not associate with human CD58 (*5*, *35*). The low-affinity and high-specificity binding characteristics of CD2 have been attributed to unusual features of its ligand-binding surface (*15*). The binding surfaces of rat and human CD2 are both relatively flat and highly charged (see Figure 1). The flatness of the surface suggests that the binding of CD2 relies less on surface-shape complementarity but rather on the spatial pattern of charges on the binding surface. 35% and 70% of the residues on the binding surfaces of rat and human CD2, respectively, are charged, compared with ∼19% for the average solvent-exposed protein surface (*36*). Mutagenesis studies of rat CD2 in which the surface residues are altered to residues with the opposite charge result in the loss of CD2 binding to CD48. For the Glu41→Arg mutant of CD2, the binding capability is restored if a residue on CD48 is similarly mutated for complementary charge reversal (CD48 Arg31→Glu), suggesting that electrostatic complementarity *may* be important to the binding interaction (*7*). Against this, the CD48 Arg31→Glu mutant on its own can still bind to wild-type CD2, indicating that it is difficult to unravel the relative contributions of charge−charge, hydrogen bond, and

van der Waals interaction forces involved. It has been argued that the charged residues contribute little to the overall binding energy due to the unfavorable effects of desolvation upon complex formation (*15*). It has therefore been proposed that these residues play a dominant role in rat CD2 ligand recognition by ensuring that the binding strength is of the appropriate magnitude (i.e., not excessively strong) while maintaining high specificity of ligand recognition. The human CD2/CD58 cocrystal structure shows that the intermolecular interface includes few hydrophobic contacts and is dominated by interdigitating charged amino acid side chains which form a complex pattern of ionic and hydrogen bond interactions (*32*).

These studies have highlighted the significance of electrostatic interactions to the function of this class of adhesion molecules. A detailed understanding of the electrostatic properties of CD2 would therefore provide invaluable insight into the high specificity and low affinity of its ligand-binding characteristics. Our previous work has suggested that there is a distinct pH dependence of rat CD2/CD48 binding in vitro (*16*). The CD2/CD48 binding appears markedly reduced below pH 6, indicating the presence of one or more titrating residues for one or both of the CD2 and CD48 binding surfaces that may be crucial in mediating the binding interaction. The determination of ionization constants by monitoring the pH-dependent chemical shifts of ^{1}H, ^{15}N, and ^{13}C NMR resonances is well-established (for a selection, see refs *37*−*43*). ^{13}C NMR in particular has been shown to be an excellent method of the accurate determination of the acid dissociation equilibria of carboxylic acids (*44*−*47*). In this study, the pH-dependent chemical shift changes of rat CD2d1 ^{13}C, ^{15}N, and ^{1}H resonances were examined in order to provide a comprehensive evaluation of the charge status of the ligand-binding surface relevant to the rationalization of the structure−activity profile of the CD2/CD48 interaction.

EXPERIMENTAL PROCEDURES

Sample Preparation. Isotope-labeled recombinant rat CD2d1 (residues 1−99) was expressed in *E. coli* expression strain BL21(DE3) using a pET-CD2 plasmid construct. The protein was purified as previously described (*48*). The purified protein was concentrated slowly due to a tendency for the CD2d1 to precipitate at high concentration, especially between the range of pH 5 and 6. The concentration of protein sample was quantified by UV absorbance measurement at 280 nm using an extinction coefficient $\epsilon_{280} = 13\,940$ M^{-1} cm^{-1} as determined by the method of (*49*) and the purity (>99%) assessed by discontinuous SDS−PAGE. Unless stated otherwise, all protein samples used for the pH titration were at a concentration of 1.2 mM in 20 mM potassium phosphate with 10% D_2O, and contained 0.5 mM EDTA and 0.1 mM PMSF. The protein samples used for the titration were initially at pH 7.5, and the pH was lowered or raised by the appropriate addition of small aliquots of 0.2 mM HCl or NaOH. The pH was measured both before and after acquisition of the NMR spectrum at each titration point, and the average of the two values was used for the analysis. The pH showed little variation at most pH titration points (±0.05 pH unit). However, above pH 8.5, where the solution is not well buffered by phosphate, the pH sometimes differed significantly before and after the experiment (up to 0.4 pH unit difference) due to an undetermined slow process. As a result of this variability, titration points at pH higher than 8.5 were not used for pK_a determination. For experiments in D_2O solution, the protein was lyophilized and then resuspended in 99.96% D_2O and the pH adjusted with aliquots of NaOD. The pH quoted for protein samples in D_2O has not been corrected for the deuterium effect on the glass electrode.

Mutagenesis. The CD2d1 mutants were constructed using a modified method of site-directed mutagenesis of Ito et al. (*50*). This method utilizes four oligonucleotides, one mutagenic primer specific for each mutagenesis reaction, and three invariant pimers for all the different mutant constructs—T7 promoter primer, T7 terminator primer (both from Novagen), and a "knock-out" primer that destroys both *Xho*I and *Bam*HI restriction sites with the sequence 5′-GAGCTC-GAATTCGGATTCTTATTCGAGAATCCTCAAG. In the first step of this modified method, the mutagenic primer was used as a forward primer for PCR together with the T7 terminator primer, while the knock-out primer was used as a reverse primer for polymerase chain reaction (PCR) together with T7 promoter primer. One microliter of the products from each PCR was used for a second round of PCR using T7 promoter and terminator primers. This DNA amplification product was then digested and inserted into the expression vector pET21b between *Nde*I and *Xho*I or *Bam*HI restriction sites. The DNA constructs were sequenced to confirm the presence of the mutations.

NMR Spectroscopy. Chemical shifts of backbone and side chain amide resonances were followed during pH titration via two-dimensional (2D) [^{15}N,^{1}H]-heteronuclear single quantum coherence (HSQC) experiments (*51, 52*). For the carboxyl resonances, a modified 2D [^{13}C,^{1}H]-H(C)CO experiment was used (*53*). However, due to severe line broadening, in particular of Glu29 and Glu41 signals, a nonconstant time version of the H(C)CO experiment was adopted for the titration. The spectra were recorded on a 600 MHz Varian UnityPlus NMR spectrometer equipped with a 5 mm triple-resonance probehead from Nalorac Cryogenics Corp. (Martinez, CA), and the data were processed using Felix version 2.3 (BIOSYM Inc., San Diego, CA) and nmrPipe (*54*). The side chain ^{13}C carboxyl resonances were assigned using a combination of 2D and 3D [^{13}C,^{1}H]-H(C)-CO spectra combined with a 2D [^{13}C,^{1}H]-H(C)CO-^{1}H-TOCSY experiment which provided connectivities between the side chain carboxyl ^{13}C′ in Asp or Glu, respectively, with the H$^{\alpha}$ proton (*53*). The [^{15}N,^{1}H]-HSQC experiments were recorded with 2048 points in F2 and 256 complex points in F1 with spectral widths of 10 000 Hz (F2) and 1700 Hz (F1). For the 2D H(C)CO experiments, the spectral width was 8000 and 2000 Hz in F2 and F1, respectively, with 2048 points in F2 and 60 complex points in F1. The number of transients recorded per t_1 increment ranged from 32 up to 400 to compensate for the line broadening of some resonances in the range 4.5 < pH < 7.5. 2D {^{1}H}-^{15}N heteronuclear nuclear Overhauser effect (NOE) experiments were measured and analyzed as described previously (*55*). All NMR experiments were performed at a temperature of 25 °C.

Determination of pK_a Values. The pK_a values of the carboxyl groups were determined by following the NMR chemical shift changes as a function of pH. The titration data for ^{13}C, ^{15}N, and ^{1}H chemical shifts (∼800 in all) were

analyzed using Mathematica (Wolfram Research) and Kaleidograph (Synergy Software). For data that showed a single titration event, the curve-fitting was performed using a nonlinear least-squares method according to the equation derived from the Henderson−Hasselbalch equation (*56*):

$$\delta = (\delta_{acid} + \delta_{base}10^{pH-pK_a})/(1 + 10^{pH-pK_a})$$

where δ is the instantaneous chemical shift in ppm, δ_{acid} is the chemical shift of the protonated form, and δ_{base} is the chemical shift of the deprotonated form. For titration data that indicated multiple protonation events and therefore did not yield a good fit to this simple relationship, the number of pK_a values used to fit the curves was increased. Fitting was done in all cases assuming that the protonation equilibria were noninteracting (*40*): each titration curve was treated as the simple sum of all individual titrating events experienced by an atom. In all cases, no more than five pK_a values were required to adequately fit the curves. In principle, it is possible to preselect the number of pK_as used to fit the curve based upon the number of charged residues present around the target atom in the three-dimensional structure. However, we opted for an unbiased method for assessing the number of pK_as required to fit a titration curve by using the *F*-statistic (*57*). The chi-square (χ^2) values obtained from each fit were used to calculate *F*-values for each change in the number of degrees of freedom associated with allowing additional titration events. The total number of degrees of freedom in the fit was assumed to be the number of titration data points (pH values), reduced by three degrees of freedom for each pK_a used in the fit (corresponding to one pK_a value and two end-point chemical shifts). The significance of the resulting *F*-value was then evaluated by reference to a normal distribution. A value of $p < 0.01$ was taken to indicate that the *F*-value is significant, and therefore the use of an increased number of pK_a values in the curve-fitting was considered justified.

Structural Analysis of CD2. The 2.8 Å resolution crystal structure of rat CD2 (Protein Data Bank code 1HNG) (*24*) was used as the template for the structural analysis. The solvent-accessible surface area of the residues in CD2 was calculated using the NACCESS program with a probe size of 1.4 Å (*58*). The hydrogen bond network was analyzed using HBPLUS (*59*).

RESULTS

NMR Resonance Assignment. The ^{1}H, ^{15}N, and ^{13}C NMR resonance assignments of CD2d1 have been reported recently (*48*) and are available at BMRB accession code 4109. Chemical shift values were deposited for three different pH values: pH 3.0, pH 5.0, and pH 7.0. The assignments include the side chain carboxyl carbon resonances of aspartic acid and glutamic acid side chains, obtained from 2D [^{1}H,^{13}C]-H(C)CO and H(C)CO-TOCSY spectra. A selected region of the 2D [^{1}H,^{13}C]-H(C)CO spectra of CD2d1 at three different pH values is shown in the Supporting Information. The resonance frequencies of most of the carboxylates lie within the expected limits. For protonated aspartic acid and glutamic acid, the carboxyl ^{13}C resonances are located between 176 and 177 ppm and 178−180 ppm, respectively, while the signals from the ionized forms are ~3−5 ppm downfield (*44*−*47*). The aspartic acid β-CH_2 protons and glutamic acid γ-CH_2 protons lie in the ranges 3.0−2.7 and 2.6−2.2 ppm, respectively, and displayed a typical upfield shift of 0.2−0.3 ppm upon carboxyl deprotonation (*47*, *60*). In contrast to this general pattern, at pH 5.0 an unusual upfield δ-carboxyl chemical shift was seen for Glu41, at a position more typical of a protonated glutamate. Similar but less pronounced chemical shift variances were also seen for Glu29, Asp28, and Asp72. These observations suggested the presence of at least one residue with an anomalously high acidity constant.

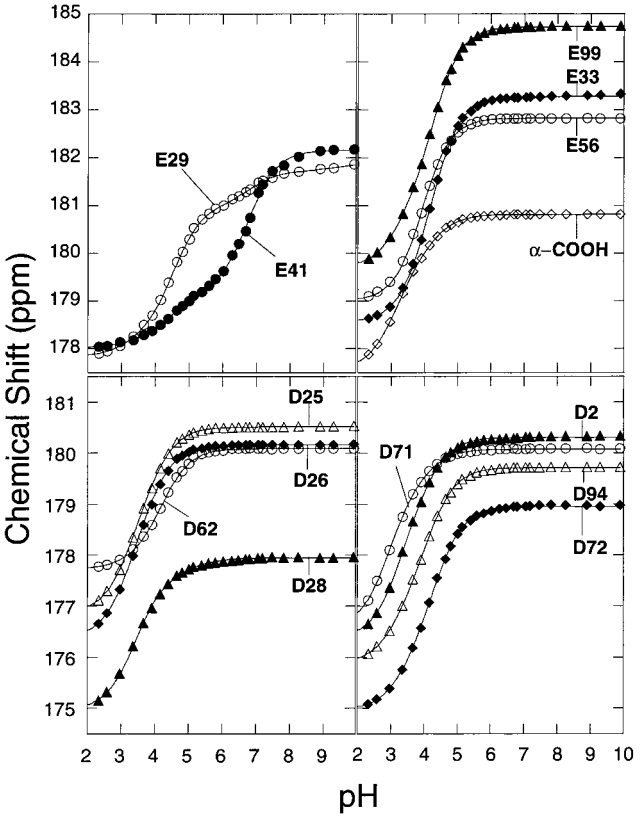

FIGURE 2: Plot of the pH variation of CD2d1 carboxyl group ^{13}C chemical shifts. The protein concentration used was 1.2 mM. The chemical shift profiles were fit to a multicomponent Henderson−Hasselbalch equation as described in the text.

pH Titration and Curve-Fitting of the 2D H(C)CO Data. 2D H(C)CO spectra were recorded at a total of 31 titration points between pH 2.0 and pH 10.0 in order to adequately sample the titration behavior of the acidic side chains. CD2d1 has five glutamic acid residues and eight aspartic acid residues as well as the C-terminal backbone carboxylate group. The pH-dependences of the chemical shifts of the carboxyl ^{13}C resonances for all of these groups are shown in Figure 2. Most of the carboxyl groups showed essentially monophasic titration behavior. A few, however, exhibited minor inflections on the titration curves and slight deviations from the monophasic model due to influences from nearby ionizable groups. For example, the data for C-terminal residue Glu99 could be curve-fit to two independent titration events with separate pK_as, which are attributed to the influence of both its side chain and its backbone carboxylate groups. The most pronounced deviation from the monophasic model can be seen in the titration curves Glu29 and Glu41, both of which show a distinct biphasic titration behavior (Figure 2).

Table 1: Acidity Constants (pK_a Values) of Acidic Groups of Rat CD2d1 Determined from 2D [^{13}C,^{1}H]-H(C)CO Experiments

	[CD2d1] = 1.2 mM			[CD2d1] = 0.1 mM	solvent accessibility (Å^2)[e]	
residue	pK_a[a]	$\Delta\delta$ (ppm)[b]	H^{β}/H^{γ}[c]	pK_a[d]	nonpolar	polar
Asp2	3.55 ± 0.04	3.77	3.46	3.48 ± 0.02	42.53	79.24
Asp25	3.53 ± 0.02	3.68	3.45, 3.61	3.50 ± 0.02	40.05	78.26
Asp26	3.58 ± 0.02	3.55	3.60, 3.55	3.57 ± 0.02	28.22	66.28
Asp28	3.57 ± 0.06	2.69	3.61, 3.96	3.53 ± 0.03	4.34	25.11
Asp62	4.15 ± 0.02	2.33	4.20, 4.19	4.02 ± 0.02	0.00	12.61
Asp71	3.18 ± 0.04	3.31	3.69, 3.01	3.30 ± 0.03	37.66	82.82
Asp72	4.14 ± 0.05	3.83	4.06, 3.82	3.97 ± 0.01	0.00	15.78
Asp94	3.87 ± 0.04	3.65	3.79	3.80 ± 0.02	8.43	35.55
Glu29	4.42 ± 0.04	2.66	4.66	4.39 ± 0.05	0.57	23.90
Glu33	4.16 ± 0.02	4.68	4.23	4.02 ± 0.01	7.45	50.67
Glu41	6.73 ± 0.05	3.00	6.88, 6.87	6.36 ± 0.02	1.91	18.73
Glu56	3.92 ± 0.01	3.80	3.99	3.74 ± 0.02	28.11	40.63
Glu99	4.25 ± 0.04	4.74	3.95	4.03 ± 0.01	77.20	99.11[f]
α-CO_2H	3.11 ± 0.05	2.30	3.49	—[g]		

[a] pK_a values were determined from the chemical shift variation of the carboxyl ^{13}C resonance of the acidic groups at a CD2d1 concentration of 1.2 mM, by curve-fitting to the Henderson−Hasselbalch equation as described in the text. If the curves indicated evidence of more than a single pK_a, only the value corresponding to the dominant $\Delta\delta$ value is given. This is taken to represent a direct measure of the intraresidue pK_a. [b] $\Delta\delta$ represents the amplitude of chemical shift differences between protonated and deprotonated forms of the carboxyl group, obtained as part of the fitting procedure. [c] pK_a values determined from the chemical shift pH profile for the methylene group protons (H^{β} for Asp residues, H^{γ} for Glu residues) adjacent to the carboxyl group. A single pK_a is reported if the methylene proton resonances are degenerate or if overlap for one these signals with the amplitude of the variation in chemical shift is too small for a meaningful fit. [d] pK_a values are reported from carboxyl ^{13}C chemical shift pH profiles obtained at a CD2d1 concentration of 0.1 mM. [e] Absolute measures of solvent-accessible surface areas were estimated from the rat CD2 crystal structure (PDB code 1HNG) using the program NACCESS and a probe size of 1.4 Å. The polar solvent accessibility corresponds to the oxygen atoms of the carboxyl group. The nonpolar surface-accessible area is computed for all other atoms of the side chain, including the C^{α} atom. [f] This value includes the terminal backbone carboxylate group. [g] Value cannot be determined due to weak peak intensities.

The pK_a values of the carboxyl groups determined from fitting the carboxyl ^{13}C chemical shifts are tabulated in Table 1. The majority of the carboxyl groups, with the notable exception of Glu41, have a pK_a similar to that expected from model compounds. For aspartates, the average observed pK_a value is ca. 3.7, which is comparable to the standard quoted value of 3.9−4.0 (*61*). For glutamate residues, the average pK_a of 4.66 is skewed by the pK_a of Glu41 which is abnormally high (see below), but nevertheless is still close to the standard value of 4.3−4.4 (*61*). There appears to be a reciprocal relationship between Glu41 and Glu29 reflected by the inflections and amplitudes of the pH chemical shift profiles obtained for these two residues (Figure 2). The unusually high pK_a of Glu41 is determined to be 6.73 ± 0.05 with an associated ^{13}C′ shift amplitude $\Delta\delta = |\delta(\text{GluH}) - \delta(\text{Glu}^-)| = 3.0$ ppm. The titration profile for Glu41 also included a more minor shift variation $\Delta\delta = 0.8$ ppm corresponding to an ionization with pK_a of 4.34 ± 0.06. The pK_a of Glu29 is determined to be 4.42 ± 0.04 associated with a major shift change $\Delta\delta = 2.8$ ppm and an additional minor $\Delta\delta = 1.0$ ppm corresponding to a pK_a of 6.73 ± 0.09. This reciprocal titration pattern of Glu41 and Glu29 is characteristic of two closely interacting carboxyl groups (*46*, *62*).

The pK_a values of the CD2d1 carboxyl groups were also determined from the pH-dependent chemical shift variation of the immediately adjacent intraresidue protons, namely, $C^{\beta}H_2$ for Asp and $C^{\gamma}H_2$ for Glu (Table 1). Most of the values obtained in this way correspond well with those obtained from the carboxyl groups (agreement to within 0.1 pH unit). However, in the case of close proximity of titrating acidic residues, the protons are subject to multiple influences that give rise to more complex titration curves that are more difficult to interpret. For example, for the pH-dependent chemical shift changes of Glu29 $C^{\gamma}H$, a slightly greater influence is exerted by the ionization of Glu41 ($\Delta\delta = 0.21$ ppm) than that from its own intraresidue carboxyl group ($\Delta\delta = 0.18$ ppm) (see figure given in Supporting Information). These observations reinforce the principle that caution should be applied when attempting to assign the identity of the residue giving rise to a specific inflection in the chemical shift vs pH profile for proton resonances of closely interacting side chains.

pK_a Determination at Low Protein Concentration. The pH titration monitored by 2D [^{1}H,^{13}C]-H(C)CO spectroscopy was repeated at a CD2d1 concentration of 0.1 mM. Overall the pattern of the ionization behavior was conserved at the lower concentration, but some small shifts in the pK_a values were observed (Table 1). For example, the pK_a of Asp28 increased by 0.10 pH unit while that of Glu56 dropped by 0.18 pH unit. Interestingly, the largest concentration-dependent change in pK_a was seen for Glu41, down from 6.74 to 6.36 (Figure 3). These changes were accompanied by some improvement in the intensity of a subset of cross-peaks in the spectrum, due to an apparent increase in transverse relaxation times. These concentration-dependent phenomena point toward possible pH-dependent protein−protein interactions at higher protein concentration (*55*).

Deuterium Isotope Shifts. The 2D H(C)CO titration results indicated that Glu41 should be mostly protonated and Glu29 deprotonated at pH ∼5.5. The protonation state of these residues was tested directly by examining the deuterium isotope effect on the carboxyl carbon chemical shift, $^{2}\Delta C^{\delta}$(OD). In general, the chemical shift of a protonated carboxyl ^{13}C resonance is shifted upfield when the solvent is changed from H_2O to D_2O. The analysis of such isotope shifts is complicated by the fact that the pH meter reading is lowered in D_2O, but at the same time acids are weaker in D_2O. To first approximation, one effect may therefore be compensated by the other, but such an assumption may not always hold. For studies in the acidic range, the pH reading can be taken as a good approximation for pD (*60*). Nevertheless, adopting

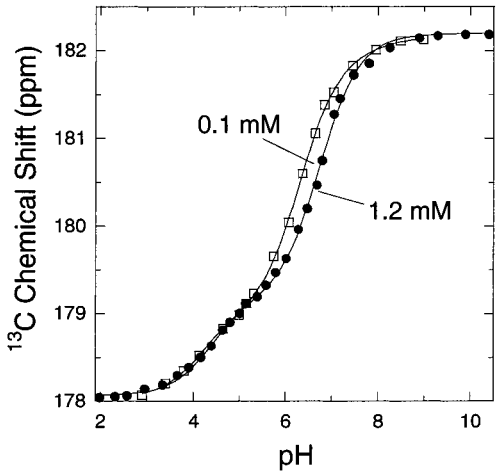

FIGURE 3: Comparison of the pH dependence of the CD2d1 Glu41 carboxyl ^{13}C resonance in titrations performed at 0.1 mM (□) and 1.2 mM (●) protein concentration. The chemical shift profiles were fit to a multicomponent Henderson−Hasselbalch equation as described in the text.

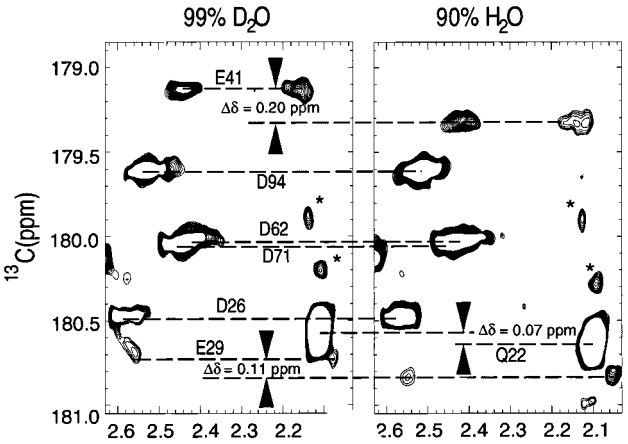

FIGURE 4: Comparison of a portion of the 2D H(C)CO spectra performed in 99% D_2O and 90% H_2O demonstrating the two-bond isotope shifts of Glu41, Glu29 [$^2\Delta C^\delta(O^\epsilon D)$], and Gln22 [$^2\Delta C^\delta$-($N^\epsilon D$)]. Peaks marked with an asterisk (*) are indirect dimension truncation artifacts.

this approach does not preclude the possibility of systematic error in the pH reading and introduction of a slight shift in derived pK_a values from the two solvent conditions (*60*, *63*). In the present case where the resonances of both Glu29 and Glu41 are very sensitive to the precise H^+ (or D^+) concentration, opportunity for experimental error enters the analysis of the deuterium isotope shift effect. The $C^\gamma H_2$ proton chemical shifts, on the other hand, are less sensitive to the deuterium isotope effect, and so these resonances were used as a reference for monitoring the pH. The 2D H(C)CO spectra of CD2 in 90% H_2O and 99% D_2O showed good alignment of $C^\gamma H_2$ proton chemical shifts at pH 5.5 (Figure 4). The chemical shifts of the majority of cross-peaks, including those from fully deprotonated aspartic acid residues, were unperturbed by the change in solvent. The chemical shift of the Gln22 C^δ carbonyl resonance was slightly perturbed, in line with expectations for the two-bond deuterium isotope shift for this type of side chain amide group, $^2\Delta C^\delta(ND) = 0.07$ ppm. In the 99% D_2O spectrum, an upfield shift $^2\Delta C^\delta(OD) = 0.20$ ppm was observed for the Glu41 carboxyl ^{13}C resonance compared to the spectrum in 90% H_2O, in line with values obtained from similar observations for protonated vs deuterated carboxyl groups (*43*, *64*, *65*). The Glu29 carboxyl showed an apparent smaller isotope shift of 0.11 ppm (Figure 4). Given the proximity of the Glu29 and Glu41 side chains in the CD2d1 structure, the presence of the Glu41 deuteron in the vicinity might lead to direct (e.g., H-bond) or indirect effects upon the Glu29 C^δ chemical shift (see Discussion).

CD2d1 pH Titration Monitored by [^{15}N,^{1}H]-HSQC Spectroscopy. The 2D [^{1}H,^{15}N]-HSQC experiment is a more rapid and economical method of studying protein ionization equilibria. We have therefore adopted this experiment to monitor the effect of salts, buffering conditions, and CD2 mutations, where preparation of ^{13}C-labeled protein samples would have been prohibitively uneconomic. For a given amide group, the ^{1}H and ^{15}N chemical shifts are very sensitive to changes in the electronic environment due to the high polarizability of N−H bonds (compared to C−H bonds) (*66*), thereby reflecting the long-range electrostatic influence of ionizable groups in the protein (*67*), as well as perturbation by pH-dependent conformational changes. The overall result is that titration curves for amide group resonances can exhibit complex titration patterns. Care must be taken in the analysis of these shift variations, in particular for titrating residues, since the dominant pK_a reflected in the ^{15}N or ^{1}H chemical shift variation need not necessarily correspond to protonation of the intraresidue side chain. However, since we had precisely established the pK_a values of all CD2d1 acidic groups via the carboxyl ^{13}C shifts, it was straightforward to correlate the pattern of titration behavior of the backbone amide resonances with these known values. For example, for wild-type CD2d1, the titration curves of the Glu29 backbone amide showed the effect of protonation of the Asp28, Glu29, and Glu41 carboxyl groups, with Asp28 exerting the greatest influence in the chemical shift changes (Figure 5). A selection of the CD2d1 pK_a values determined from chemical shift variation in the 2D [^{15}N,^{1}H]-HSQC titrations is tabulated in the Supporting Information. The protonation of Glu41 with a p$K_a \sim 6.7$ gives rise to readily detectable chemical shift effects on Asp28 (H^N resonance), Glu29 (H^N and N), Glu41(H^N), Lys43 (N), Ser52-(N), and Thr79(N) (Figure 5). In addition to backbone amide groups, the titration characteristics of side chain N−H cross-peaks (e.g., Arg31, Arg70, Arg90, Asn17, Asn60) also proved valuable, with downfield ^{1}H titration shifts (∼0.2−0.5 ppm) giving indications of transient side chain H-bonding interaction with acidic residues (*68*). For example, the titration profile for the Arg31 H^ϵ signal exhibited a biphasic curve corresponding to measured pK_a values of 6.68 ($\Delta\delta$ = 0.2 ppm) and 4.24 ($\Delta\delta = 0.5$ ppm) which respectively reflect the ionizations of Glu41 and Glu29 at adjacent sites in the structure (Figure 1). Collectively these backbone and side chain groups therefore proved a reliable probe of the protonation status of Glu41 as a function of different sample conditions, and point mutation of CD2d1 (see Table 2).

pH Titrations with Different Buffer Conditions. Protein pK_a values can be strongly influenced by the ionic strength and the choice of buffer (*67*, *69*). In general, larger perturbations from model compound pK_a values might be expected at low ionic strength (*70*). The [^{15}N,^{1}H]-HSQC pH titration of CD2d1 was repeated in phosphate buffer with high salt concentrations (100 and 300 mM NaCl) to probe the effect of ionic strength (Figure 5A), and an additional titration was

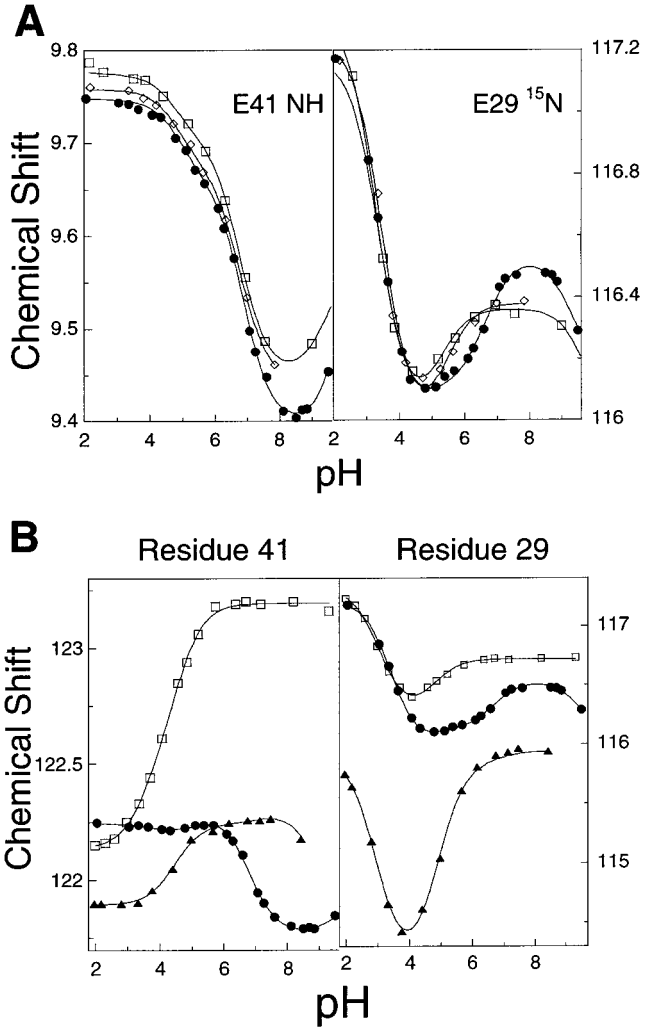

FIGURE 5: pH-dependent chemical shifts of selected backbone amide resonances. (A) Comparison of the chemical shift pH titration profiles for the amide H^N proton of Glu41 and the amide ^{15}N resonance of Glu29 illustrating the effect of increasing ionic strength. The experiments were performed in 20 mM phosphate buffer with no added salt (●), 100 mM added NaCl (◇), and 300 mM NaCl (□). (B) Comparison of the pH titration curves for the amide ^{15}N chemical shift of residues 29 and 41 for wild-type (Glu41 and Glu29) CD2d1 (●), and for the E41Q (□) and E29Q (▲) CD2d1 mutants.

performed in 10 mM Bis-tris buffer in order to ascertain whether the anomalous pK_a of Glu41 is an artifact of specific ion (e.g., phosphate) binding. With few exceptions, the titration patterns of all the amides were little changed at higher salt concentration, with only small shifts in the observed pK_a values (see Table 2 and Supporting Information). The largest shift in pK_a was seen for the resonances of Asn60 which at low ionic strength report on the pK_a of Asp62. This pK_a dropped from 4.4 at low ionic strength to 4.0 at 300 mM NaCl. The anomalous pK_a of Glu41, however, remained unaffected at the higher ionic strength conditions (see Table 2) where there was screening of charge−charge interactions. This result suggests that the short-range interaction that exists between Glu29 and Glu41 may therefore comprise a component which is not purely electrostatic in origin. The pH titration experiment was also repeated in 10 mM Bis-tris buffer. The pK_a values of most of the acidic residues appeared to be largely unchanged, with only slight shifts observed (see Supporting Information). In particular,

Table 2: Acidity Constants (pK_a Values) for Rat CD2d1 Residues Glu29 and Glu41 Determined from pH Titration Monitored by 2D [^{15}N,^1H]-HSQC Experiments[a]

	pK_a value[c]					
residue[b]	no added NaCl	100 mM NaCl	300 mM NaCl	10 mM Bis-tris	E41Q CD2d1	E29Q CD2d1
Glu29[d]	4.9	4.9 ± 0.1	4.7 ± 0.1	4.7 ± 0.1	4.5 ± 0.1	N/A
Glu41[d]	6.8 ± 0.2	6.7 ± 0.1	6.7 ± 0.1	6.7 ± 0.1	N/A	5.0 ± 0.1

[a] Effect of buffer conditions and point mutations. [b] Mean values of the pK_a values were derived from the averaging of the separate fits of chemical shift pH profiles for multiple cross-peaks. Chemical shift pH profiles were fit to the Henderson−Hasselbalch equation as described in the text. Full details of the set of pK_a values determined from the 2D [^{15}N,^1H]-HSQC pH titration data are given in the Supporting Information. N/A: not applicable. [c] pK_a values were determined for wild-type CD2d1 at varying salt and buffer conditions as indicated, and separately for the E41Q and E29Q CD2d1 mutants at low ionic strength. All titrations were performed in 20 mM phosphate except for the experiment in 10 mM Bis-tris buffer. [d] Inflections in the pH−chemical shift profiles unambiguously attributable to the ionization of Glu29 were observed for the following resonances: Glu41 H^N, Lys43 N. The corresponding signals used for the estimation of the Glu41 pK_a were the following: Asp28 H^N, Glu 29 H^N, Glu29 N, Glu41 H^N, Lys43 N, Ser52 N, and Thr79 N. Only those changes which give rise to chemical shift amplitudes $\Delta\delta > 0.05$ ppm for H^N protons and $\Delta\delta > 0.5$ ppm for ^{15}N chemical shifts were included.

no significant difference was observed in the pK_a of Glu41, which remained at ∼6.7, indicating that the unusual acidity constant of this residue is not the result of specific ion binding effects (Table 2).

Mutant Studies. To confirm the residue assignment of the anomalous pK_a, Glu41 was mutated to glutamine (E41Q CD2d1), a change which removes the charge while maintaining the overall shape and bulk of the side chain. The backbone amide resonances of the E41Q mutant did not show significant changes in chemical shift at low pH, indicating that at low pH the protein fold and the disposition of the side chains are largely unaltered. The assignment of the NMR cross-peaks for the ^{15}N-labeled CD2d1 E41Q mutant was therefore straightforward. Furthermore, the pH titration curves obtained for the E41Q mutant, with only a few exceptions such as that of the Gln41 substitution (Figure 5B), are nearly identical compared to wild-type CD2 in the range pH 2−5. The most significant change observed in the titration of the E41Q mutant is the dramatic abolition of the shifts which were seen for several wild-type CD2d1 resonances between pH 5.5−7.5. This result reinforces the attribution of the anomalous pK_a of wild-type CD2d1 to Glu41. A second mutant of CD2d1, in which Glu29 was similarly mutated to a glutamine (E29Q CD2d1), was also characterized in a [^{15}N,^1H]-HSQC pH titration (Figure 5B). Selected pK_a values derived from the examination of these two CD2d1 mutants are listed in Table 2; a more complete compilation is given in the Supporting Information. Compared to wild-type CD2d1, the most notable change in these values is the reduction of the pK_a value of Glu41 by ca. 1.7 units to pK_a ∼ 5.0 in E29Q CD2d1. This result suggests that a major contributing factor to the elevated pK_a of Glu41 in wild-type CD2 is the presence of deprotonated Glu29 in an adjacent location on the major β-sheet surface.

Heteronuclear NOE Experiments. A series of 2D heteronuclear {^1H}-^{15}N NOE experiments were performed to examine the mobility of the CD2d1 arginine side chains as

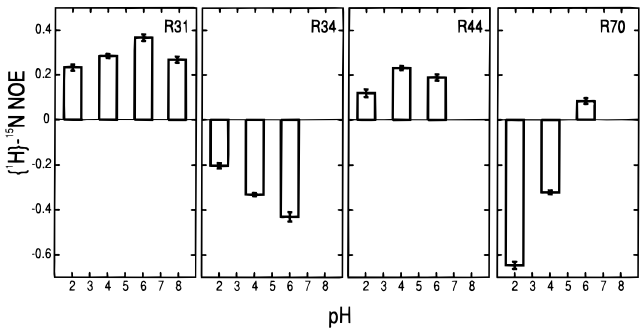

FIGURE 6: Heteronuclear {^{1}H}-^{15}N NOE values of selected CD2d1 arginine side chain N$^\epsilon$H groups at different pH values. The pH profiles of the heteronuclear NOE values for the side chains of Arg87 and Arg96 (not shown) are similar to that of Arg34.

a function of the sample pH. The pH variation of the heteronuclear NOE for some selected Arg N$^\epsilon$H groups is displayed in Figure 6. A negative value of the heteronuclear NOE is indicative of a high degree of side chain flexibility while a positive NOE suggests some degree of restriction of the internal motion. Figure 6 shows that there are clearly very different characteristics for different Arg side chains. With the exception of Arg1 in the unstructured N-terminus, all the Arg N$^\epsilon$H cross-peaks were readily detectable in the spectra from pH 2.0 to pH 6.0. At higher pH values, the majority of these peaks are lost due to rapid solvent exchange. The N$^\epsilon$H cross-peak of Arg31, however, did not show significant solvent exchange broadening until pH 8.5 and displayed the highest heteronuclear NOE values at all pH titration points studied. This observation suggests that the Arg31 N$^\epsilon$H group is protected from exchange by hydrogen bonding (perhaps to neighboring residues Glu29 and Glu41; see Figure 1) or partial burial (*71*). The only other Arg residue with consistently positive N$^\epsilon$H heteronuclear NOE values was Arg44, which could reflect hydrogen bonding to the backbone carbonyl of Ile27 (as seen in the crystal structure), as well as interactions with Asp25 and Asp28. The N$^\epsilon$H heteronuclear NOE values of Arg34, Arg87, and Arg96 were consistently negative across the pH range which indicates that they experience relatively little motional restriction. The side chain of Arg70, while completely flexible at low pH, showed a rising trend in heteronuclear NOE values with pH that indicates decreasing flexibility, most likely as a result of the formation of a salt bridge interaction with deprotonated Glu99.

DISCUSSION

It emerged from the analysis of the protonation equilibria for rat CD2d1 that the side chain carboxyl of Glu41 exhibits an anomalous acidity constant. The pK_a of the Glu41 was determined from direct measurements of the carboxyl ^{13}C chemical shifts to be 6.73 ± 0.05, which is unusually elevated for a glutamic acid residue, and is particularly surprising in light of its position on the surface of the protein (Figure 1). The attribution of this pK_a to Glu41 is supported by analysis of the two-bond deuterium isotope shifts that demonstrate Glu41 to be protonated at pH 5.5 (Figure 4). Further confirmation of this assignment comes from site-directed mutagenesis whereby mutation of Glu41 to glutamine completely abolished the backbone amide chemical shift changes previously seen for several resonances in wild-type CD2d1 between pH 5.5 and 7.5, which derive from the vicinity of the Glu41 side chain on the major β-sheet ligand-binding face of the domain. The precise value of the acidity constant for Glu41 is slightly dependent upon protein concentration (Figure 3), which suggests that the self-association of the protein may account for a minor component of the elevation of the pK_a value. It has recently been shown that rat CD2d1 dimerizes weakly at pH 6.0 with a $K_D \sim 5$ mM, so at 1.2 mM concentration less than ~30% of CD2d1 is in a dimer state (*55*). Self-association at this concentration is strongly pH-dependent and is near-maximal at pH 6.0; no self-association is detectable at pH <4 (unpublished observations). At a concentration of 0.1 mM, essentially all of the molecules are in the monomer state, in which the Glu41 acidity constant retains an elevated value, p$K_a \sim 6.4$. Therefore, the molecular origin for the unusual characteristics of this side chain is not directly related to self-association of the protein and therefore must be sought in features of the monomeric protein structure.

Unusual pK_a values have often been observed for many residue types in a variety of proteins; these normally reside within an active site and are implicated in catalytic function (*72, 73*). They can also be found at ligand-binding sites (*74*) as well as at points of protein−protein contact (*75*). Such unusual pK_a values may be the product of a number of factors, such as charge−charge interactions between ionizable groups, the effect of protein binding to specific buffer components, and the degree of solvent accessibility of charged side chains (*69, 76*). For CD2d1, no specific ion effect from the buffer used was observed (Table 2), and the elevated pK_a of Glu41 is therefore a consequence of this residue's microscopic physicochemical environment. The ligand-binding site of CD2d1 comprises a cluster of exposed charged residues on the major β-sheet, including Glu41 (see Figure 1). It is to be expected that side chains on this surface will interact strongly with each other. The clear outcome of our studies is that Glu29 exhibits evidence of interactions with Glu41, as indicated by the biphasic nature and reciprocal relationship of these residues' pH titration curves (Figure 2), and the observation that the pK_a of Glu41 is strongly depressed (from 6.7 to ca. 5.0) in the E29Q mutant of CDd21 (Table 2). Similar examples of coupled titration behavior have been observed for ribonuclease H1 (*46*) and *Bacillus circulan* xylanase (*62*), where the effects on the pK_a values were analyzed on the basis of consideration of the mutual electrostatic repulsion of the acidic residues. Examination of the 2.8 Å resolution crystal structure of rat CD2 reveals that the side chain methylene groups of Glu41 and Glu29 are in van der Waals contact, and the carboxyl groups are positioned such that charge−charge repulsion would be very strong. The carboxyl C$^\delta$ atoms of these two residues are separated by a distance of only ~5.6 Å. The positive heteronuclear NOE values for the neighboring Arg31 and Arg44 N$^\epsilon$H groups (Figure 6) and the nondegeneracy of the C$^\gamma$H$_2$ proton resonances of Glu41 and Glu29 suggest that the side chains of residues surrounding Glu41 have only limited mobility, probably as a result of being held in position by complex electrostatic interactions between the many charged groups on this surface. As a result, the two glutamates are prevented from rotating away from each under the force of electrostatic repulsion. Two other carboxyl groups, Glu33 and Asp28, are also close to Glu41 and, by

electrostatic repulsion, may contribute in a minor way to the elevation of the pK_a for this residue. There are two basic groups (Arg31 and Lys43) located immediately adjacent to Glu41 that could also have a strong influence. Any pairing of these groups with Glu41, however, would be expected to lower, rather than raise, the Glu41 pK_a by charge attraction (*77*, *78*). It is intriguing that the proximity of Glu29 to Glu41 dominates the effects of these positively charged side chains. The closest approach of the carboxyl O^{ϵ} atoms of Glu41 and Glu29 is ~2.9 Å, which is sufficiently close for a hydrogen bond to be formed between a protonated Glu41 and a deprotonated Glu29, a scenario which is consistent with the elevation of the pK_a of Glu41 and might suggest a physical basis for the 0.11 ppm deuterium isotope shift observed for the Glu29 carboxyl ^{13}C resonance (Figure 4). It is notable that the coupling of Glu41 and Glu29 does not lead to a substantial perturbation of the pK_a of the latter residue. In the crystal structure of rat CD2, the closest approaches to the Glu29 carboxyl group by the ζ-amino group of Lys43, the guanidino group of Arg31, and the carboxyl group of Asp28 are 2.9, 4.5, and 5.2 Å, respectively (Figure 1). Presumably, in contrast to the situation for Glu41, the balance of additional side chains with positive and negative charges in the immediate vicinity, together with its own relatively low solvent accessibility (Table 1), leads to an overall neutral effect on Glu29.

The extent of burial of charged groups can be a significant contributory factor in determining pK_a values (*78*). The data presented in Table 1 for CD2d1 indicate some correlation between solvent accessibility and the pK_a. For example, among the aspartic acid residues, Asp62 and Asp72 showed both the lowest degree of solvent accessibility and the highest pK_a values—4.15 and 4.14, respectively, compared with an average of 3.55 for the remainder. The Asp62 and Asp72 acidity constants are not unusually elevated, but it is interesting to note that in the CD2 crystal structure each of these side chains forms a hydrogen bond with the backbone amide of Ile18 and Thr69, respectively. Such hydrogen bonding would be expected to have the effect of lowering the pK_a, as has been observed for the hydrogen-bonded carboxyl groups of other proteins (*41*, *43*, *77*). The absence of such a lowering of the acidity constants for these residues in CD2 suggests that such H-bonding is more than compensated by factors that favor the raising of the pK_a, such as reduced side chain solvent accessibility.

The present results suggest that unusually perturbed pK_a values may arise for proteins in solution, the basis for which is not apparent from cursory inspection of their three-dimensional structures. Certainly even when it became evident that CD2d1 possessed a residue with an unexpected acidity constant, we were unable to identify Glu41 by a priori inspection of the CD2 crystal structure, nor were we able to obtain an unambiguous prediction for this assignment with protein pK_a prediction software (unpublished observations). It has been possible to identify Glu41 as the origin of the anomalous pK_a, and Glu29 as the major contributing influence, but only through this careful experimental analysis by NMR and mutagenesis.

The unusually elevated pK_a of Glu41 raises an interesting question about this residue's protonation state and its role in ligand-binding interactions. Davis et al. (*5*) proposed that the CD2/CD48 interaction is primarily mediated by hydrophobic residues on the CD2 binding surface such as Leu38, Phe49, and Tyr81 while the charged residues contribute little binding energy to the interaction. The role played by the charged residues was postulated primarily to provide the specificity of ligand binding without a concomitant increase in binding strength, thereby maintaining the low affinity necessary for the transient and reversible interaction of the T-cell with other tissues. It has been separately argued from a comparison of the proposed ligand-binding sites of human and rat CD2 that the species- and ligand-specific binding may be determined by just three residues: Thr37, Leu38, and Glu41 (*16*). The involvement of Glu41 in the binding interaction has been tested in a number of mutagenesis studies. Charge reversal mutation of Glu41→Arg abrogated CD2 binding to CD48; complementary charge reversal mutagenesis of CD48 residue Arg31→Glu restored the binding capability (*7*). A CD2 Glu41→Ala mutant, however, could tolerate drastic substitution at Arg31 of CD48 and is promiscuous in being able to bind to many CD48 variants at this site. These results were taken as an indication that the charge of Glu41 has the primary role of conferring ligand specificity to the interaction of CD2 with CD48 (*15*). It is interesting to consider whether the anomalous ionization properties of CD2 Glu41 observed in the free form of the protein would be retained in the complex formed with CD48. In this context, it is noteworthy that the corresponding residue in the structure of human CD2 (Gln46) is uncharged and resides at the center of the CD2/CD58 interface revealed by the cocrystal structure of these proteins (*32*). The Gln46 side chain in human CD2 sits opposite Leu27 on CD58, representing an 'island' of nonpolar contacts surrounded by polar and ionic salt bridge interactions. If the structure of the rat CD2/CD48 complex is highly homologous to human CD2/CD58, then Glu41 of rat CD2 would be sited opposite Thr33 on CD48, and only obliquely juxtaposed with the proposed salt bridge partner Arg31 on CD48 (*7*). A previous study reported a marked reduction in the binding of CD2 to CD48 below pH ~6 (*16*), thereby implicating the presence of one or more ionizable residues in the binding interface region with a corresponding pK_a ~ 6. Thus, while it may be that Glu41 is deprotonated in the functional complex of rat CD2 with CD48, the anomalous pK_a of Glu41 suggests that this residue should be considered a candidate to rationalize the pH-dependent properties of this interaction. Whether the anomalously high pK_a of Glu41 described here and the pH-dependent binding behavior of CD2 has any bearing on the function of CD2 in vivo remains to be established.

In summary, the electrostatic properties of the binding surface are crucial to the definition of the binding affinity and ligand specificity of the adhesion properties of CD2, and changes in pH can have a significant effect on the strength of binding. These observations will prove useful in the rationalization of the structure—activity profile of this component of the molecular T-cell/antigen-presenting cell adhesion system, particularly in light of ongoing investigations of the complex of rodent CD2/CD48 complexes. In addition, these pK_a measurements should provide a useful target for developers of the theoretical analysis of the electrostatic properties of proteins (*79*).

ACKNOWLEDGMENT

We thank Dr. P. Anton van der Merwe and Dr. Simon J. Davis (University of Oxford) for valuable discussions.

SUPPORTING INFORMATION AVAILABLE

Data for a selected region of the 2D [^{1}H,^{13}C]-H(C)CO spectra of CD2d1 at three different pH values (7 pages). This material is available free of charge via the Internet at http://pubs.acs.org.

REFERENCES

1. Moingeon, P., Chang, H. C., Sayre, P. H., Clayton, L. K., Alcover, A., Gardner, P., and Reinherz, E. L. (1989) *Immunol. Rev. 111*, 111−144.
2. Bierer, B. E., Sleckman, B. P., Ratnofsky, S. E., and Burakoff, S. J. (1989) *Annu. Rev. Immunol. 7*, 579−599.
3. Springer, T. A. (1990) *Nature 346*, 425−434.
4. Davis, S. J., and van der Merwe, P. A. (1996) *Immunol. Today 17*, 177−187.
5. Davis, S. J., Ikemizu, S., Wild, M. K., and van der Merwe, P. A. (1998) *Immunol. Rev. 163*, 217−236.
6. Monks, C. R. F., Freiberg, B. A., Kupfer, H., Sciaky, N., and Kupfer, A. (1998) *Nature 395*, 82−86.
7. van der Merwe, P. A., McNamee, P. N., Davies, E. A., Barclay, A. N., and Davis, S. J. (1995) *Curr. Biol. 5*, 74−84.
8. Dustin, M. L., Olszowy, M. W., Holdorf, A. D., Li, J., Bromley, S., Desai, N., Widder, P., Rosenberger, F., van der Merwe, P. A., Allen, P. M., and Shaw, A. S. (1998) *Cell 94*, 667−677.
9. Sunder-Plassmann, R., and Reinherz, E. L. (1998) *J. Biol. Chem. 273*, 24249−24257.
10. Kato, K., Koyanagi, M., Okada, H., Takanashi, T., Wong, Y. W., Williams, A. F., Okumura, K., and Yagita, H. (1992) *J. Exp. Med. 176*, 1241−1249.
11. van der Merwe, P. A., McPherson, D. C., Brown, M. H., Barclay, A. N., Cyster, J. G., Williams, A. F., and Davis, S. J. (1993) *Eur. J. Immunol. 23*, 1373−1377.
12. Hunig, T. (1985) *J. Exp. Med. 162*, 890−901.
13. Selvaraj, P., Plunkett, M. L., Dustin, M., Sanders, M. E., Shaw, S., and Springer, T. A. (1987) *Nature 326*, 400−403.
14. van der Merwe, P. A., and Barclay, A. N. (1994) *Trends Biochem. Sci. 19*, 354−358.
15. Davis, S. J., Davies, E. A., Tucknott, M. G., Jones, E. Y., and van der Merwe, P. A. (1998) *Proc. Natl. Acad. Sci. U.S.A. 95*, 5490−5494.
16. McAlister, M. S. B., Mott, H. R., van der Merwe, P. A., Campbell, I. D., Davis, S. J., and Driscoll, P. C. (1996) *Biochemistry 35*, 5982−5991.
17. Pierres, A., Benoliel, A. M., Bongrand, P., and van der Merwe, P. A. (1996) *Proc. Natl. Acad. Sci. U.S.A. 93*, 15114−15118.
18. Dustin, M. L., Golan, D. E., Zhu, D. M., Miller, J. M., Meier, W., Davies, E. A., and van der Merwe, P. A. (1997) *J. Biol. Chem. 272*, 30889−30898.
19. Dustin, M. L. (1997) *J. Biol. Chem. 272*, 15782−15788.
20. Silkowski, H., Davis, S. J., Barclay, A. N., Rowe, A. J., Harding, S. E., and Byron, O. (1997) *Eur. Biophys. J. Biophys. Lett. 25*, 455−462.
21. Peterson, A., and Seed, B. (1987) *Nature 329*, 842−846.
22. Sayre, P. H., Hussey, R. E., Chang, H. C., Ciardelli, T. L., and Reinherz, E. L. (1989) *J. Exp. Med. 169*, 995−1009.
23. Hahn, W. C., Menu, E., Bothwell, A. L. M., Sims, P. J., and Bierer, B. E. (1992) *Science 256*, 1805−1807.
24. Jones, E. Y., Davis, S. J., Williams, A. F., Harlos, K., and Stuart, D. I. (1992) *Nature 360*, 232−239.
25. Bodian, D. L., Jones, E. Y., Harlos, K., Stuart, D. I., and Davis, S. J. (1994) *Structure 2*, 755−766.
26. Driscoll, P. C., Cyster, J. G., Campbell, I. D., and Williams, A. F. (1991) *Nature 353*, 762−765.
27. Withka, J. M., Wyss, D. F., Wagner, G., Arulanandam, A. R. N., Reinherz, E. L., and Recny, M. A. (1993) *Structure 1*, 69−81.
28. Williams, A. F., and Barclay, A. N. (1988) *Annu. Rev. Immunol. 6*, 381−405.
29. Wong, Y. W., Williams, A. F., Kingsmore, S. F., and Seldin, M. F. (1990) *J. Exp. Med. 171*, 2115−2130.
30. Davis, S. J., Davies, E. A., and van der Merwe, P. A. (1995) *Biochem. Soc. Trans. 23*, 188−194.
31. Sun, Z. Y. J., Dotsch, V., Kim, M., Li, J., Reinherz, E. L., and Wagner, G. (1999) *EMBO J. 18*, 2941−2949.
32. Wang, J., Smolyar, A., Tan, K. M., Liu, J., Kim, M. Y., Sun, Z. J., Wagner, G., and Reinherz, E. L. (1999) *Cell 97*, 791−803.
33. van der Merwe, P. A., Barclay, A. N., Mason, D. W., Davies, E. A., Morgan, B. P., Tone, M., Krishnam, A. K. C., Ianelli, C., and Davis, S. J. (1994) *Biochemistry 33*, 10149−10160.
34. van der Merwe, P. A., Brown, M. H., Davis, S. J., and Barclay, A. N. (1993) *EMBO J. 12*, 4945−4954.
35. Somoza, C., Driscoll, P. C., Cyster, J. G., and Williams, A. F. (1993) *J. Exp. Med. 178*, 549−558.
36. Miller, S., Janin, J., Lesk, A. M., and Chothia, C. (1987) *J. Mol. Biol. 196*, 641−656.
37. Bradbury, J. H., and Scheraga, H. A. (1966) *J. Am. Chem. Soc. 88*, 4240.
38. Ebina, S., and Wuthrich, K. (1984) *J. Mol. Biol. 179*, 283−288.
39. Kohda, D., Sawada, T., and Inagaki, F. (1991) *Biochemistry 30*, 4896−4900.
40. Forman-Kay, J. D., Clore, G. M., and Gronenborn, A. M. (1992) *Biochemistry 31*, 3442−3452.
41. Schaller, W., and Robertson, A. D. (1995) *Biochemistry 34*, 4714−4723.
42. Khare, D., Alexander, P., Antosiewicz, J., Bryan, P., Gilson, M., and Orban, J. (1997) *Biochemistry 36*, 3580−3589.
43. Joshi, M. D., Hedberg, A., and McIntosh, L. P. (1997) *Protein Sci. 6*, 2667−2670.
44. Richarz, R., and Wuthrich, K. (1978) *Biochemistry 17*, 2263−2269.
45. Qin, J., Clore, G. M., and Gronenborn, A. M. (1996) *Biochemistry 35*, 7−13.
46. Oda, Y., Yamazaki, T., Nagayama, K., Kanaya, S., Kuroda, Y., and Nakamura, H. (1994) *Biochemistry 33*, 5275−5284.
47. Jeng, M. F., and Dyson, H. J. (1996) *Biochemistry 35*, 1−6.
48. Chen, H. A., Pfuhl, M., Davis, B., and Driscoll, P. C. (1998) *J. Biomol. NMR 12*, 457−458.
49. Gill, S. C., and von Hippel, P. H. (1989) *Anal. Biochem. 182*, 319−326.
50. Ito, W., Ishiguro, H., and Kurosawa, Y. (1991) *Gene 102*, 67−70.
51. Norwood, T. J., Boyd, J., Soffe, N., and Campbell, J. D. (1990) *J. Am. Chem. Soc. 112*, 9638−9640.
52. Bax, A., Ikura, M., Kay, L. E., Torchia, D. A., and Tschudin, R. (1990) *J. Magn. Reson. 86*, 304−318.
53. Zhang, W. X., and Gmeiner, W. H. (1996) *J. Biomol. NMR 7*, 247−250.
54. Delaglio, F., Grzesiek, S., Vuister, G. W., Zhu, G., Pfeifer, J., and Bax, A. (1995) *J. Biomol. NMR 6*, 277−293.
55. Pfuhl, M., Chen, H. A., Kristensen, S., and Driscoll, P. C. (1999) *J. Biomol. NMR 14*, 307−320.
56. Edsel, J. T., and Wyman, J. (1958) *Biophysical Chemistry*, Academic Press, New York.
57. Kinney, J. J. (1997) *Probability—an introduction with statistical applications*, John Wiley & Sons, Inc., New York.
58. Hubbard, S. J., Campbell, S. F., and Thornton, J. M. (1991) *J. Mol. Biol. 220*, 507−530.
59. McDonald, I. K., and Thornton, J. M. (1994) *J. Mol. Biol. 238*, 777−793.
60. Bundi, A., and Wuthrich, K. (1979) *Biopolymers 18*, 285−297.
61. Creighton, T. E. (1993) *Proteins—Structures and Molecular Properties*, 2nd ed., W. H. Freeman and Co., New York.
62. McIntosh, L. P., Hand, G., Johnson, P. E., Joshi, M. D., Korner, M., Plesniak, L. A., Ziser, L., Wakarchuk, W. W., and Withers, S. G. (1996) *Biochemistry 35*, 9958−9966.
63. Led, J. J., and Petersen, S. B. (1979) *J. Magn. Reson. 33*, 603−617.

64. Ladner, H. K., Led, J. J., and Grant, D. M. (1975) *J. Magn. Reson. 20*, 530−534.
65. Wang, Y. X., Freedberg, D. I., Yamazaki, T., Wingfield, P. T., Stahl, S. J., Kaufman, J. D., Kiso, Y., and Torchia, D. A. (1996) *Biochemistry 35*, 9945−9950.
66. de Dios, A. C., Pearson, J. G., and Oldfield, E. (1993) *Science 260*, 1491−1496.
67. Russell, A. J., and Fersht, A. R. (1987) *Nature 328*, 496−500.
68. Szyperski, T., Antuch, W., Schick, M., Betz, A., Stone, S. R., and Wüthrich, K. (1994) *Biochemistry 33*, 9303−9310.
69. Matthew, J. B., Gurd, F. R. N., Garciamoreno, E. B., Flanagan, M. A., March, K. L., and Shire, S. J. (1985) *CRC Crit. Rev. Biochem. 18*, 91−197.
70. Tan, Y. J., Oliveberg, M., Davis, B., and Fersht, A. R. (1995) *J. Mol. Biol. 254*, 980−992.
71. Pascal, S. M., Yamazaki, T., Singer, A. U., Kay, L. E., and Forman-Kay, J. D. (1995) *Biochemistry 34*, 11353−11362.
72. Fersht, A. (1985) *Enzyme Structure and Mechanism*, 2nd ed., W. H. Freeman and Co., New York.
73. Nakamura, H. (1996) *Q. Rev. Biophys. 29*, 1−90.
74. Yu, L. P., and Fesik, S. W. (1994) *Biochim. Biophys. Acta 1209*, 24−32.
75. Andersen, J. F., Sanders, D. A. R., Gasdaska, J. R., Weichsel, A., Powis, G., and Montfort, W. R. (1997) *Biochemistry 36*, 13979−13988.
76. Honig, B., and Nicholls, A. (1995) *Science 268*, 1144−1149.
77. Baker, W. R., and Kintanar, A. (1996) *Arch. Biochem. Biophys. 327*, 189−199.
78. Dillet, V., Dyson, H. J., and Bashford, D. (1998) *Biochemistry 37*, 10298−10306.
79. Warshel, A., and Papazyan, A. (1998) *Curr. Opin. Struct. Biol. 8*, 211−217.

BI992209Z